First observation-based estimates of cloud-free aerosol radiative forcing across China

Zhanqing Li,[1,2,3] Kwon-Ho Lee,[1,4] Yuesi Wang,[2] Jinyuan Xin,[2] and Wei-Min Hao[5]

Received 5 October 2009; revised 19 February 2010; accepted 26 April 2010; published 4 September 2010.

[1] Heavy loading of aerosols in China is widely known, but little is known about their impact on regional radiation budgets, which is often expressed as aerosol radiative forcing (ARF). Cloud-free direct ARF has either been estimated by models across the region or determined at a handful of locations with aerosol and/or radiation measurements. In this study, ARF is determined at 25 stations distributed across China where aerosol optical thickness has been measured since 2004. In combination with the single-scattering albedo retrieved from ground and satellite measurements, ARF was determined at all the stations at the surface, inside the atmosphere, and at the top of atmosphere (TOA). Nationwide annual and diurnal mean ARF is found to be -15.7 ± 8.9 at the surface, 0.3 ± 1.6 at the TOA, and 16.0 ± 9.2 W m^{-2} inside the atmosphere. These values imply that aerosols have very little impact on the atmosphere-surface system but substantially warm up the atmosphere at the expense of cooling the surface. The strong atmospheric absorption is likely to alter atmospheric thermodynamic conditions and thus affects circulation considerably.

Citation: Li, Z., K.-H. Lee, Y. Wang, J. Xin, and W.-M. Hao (2010), First observation-based estimates of cloud-free aerosol radiative forcing across China, *J. Geophys. Res.*, *115*, D00K18, doi:10.1029/2009JD013306.

1. Introduction

[2] Atmospheric aerosols affect the climate system by reflecting, absorbing, and scattering electromagnetic radiation and by serving as cloud condensation nuclei, which further influences global energy and hydrologic cycles [*Charlson et al.*, 1992; *Ramanathan et al.*, 2001a; *Kaufman et al.*, 2005]. Depending on their composition, aerosols can absorb a substantial amount of solar radiation [*Li*, 1998; *Ramanathan et al.*, 2007], leading to a warming of the atmosphere and cooling of the surface. Black carbon or soot particles were shown to contribute to global warming [*Hansen et al.*, 2000; *Jacobson*, 2001] and to alter rainfall patterns in China and India [*Menon et al.*, 2002].

[3] Aerosol radiative forcing (ARF), a measure of the amount of radiative energy altered by aerosols, remains one of the most uncertain forcings to the climate system [*Intergovernmental Panel on Climate Change*, 2007]. This is because aerosols vary considerably with time and space with a variety of shapes and composition. To estimate global ARF requires continuous observations of aerosol loading and optical properties from satellites, ground-based networks, and dedicated field experiments.

[4] Many investigations have been made to characterize atmospheric aerosols and their radiative effects around the world, as recently reviewed by *Yu et al.* [2009]. Studies focusing on Asia include, among others, the Indian Ocean Experiment (INDOEX) [*Ramanathan et al.*, 2001b], the Asian Pacific Regional Aerosol Characterization Experiment (ACE-Asia) [*Huebert et al.*, 2003], the Asian Atmospheric Particle Environment (APEX) [*Nakajima et al.*, 2003], and the East Asian Study of Tropospheric Aerosols: An International Regional Experiment (EAST-AIRE) [*Li et al.*, 2007a].

[5] During the EAST-AIRE field campaign, extensive measurements of aerosol optical, physical, and chemical properties over China were acquired, which are essential in understanding their effects on climate. Since the beginning of the experiment in 2004, some important milestones have been reached. A nationwide look at the distribution of aerosol optical thickness (AOT, τ) [*Xin et al.*, 2007] and aerosol single-scattering albedo (SSA) [*Lee et al.*, 2007; *Zhao and Li*, 2007] was made, as well as an estimation of aerosol radiative forcing at a couple of super sites [*Li et al.*, 2007b; *Xia et al.*, 2007]. These allow us to determine the spatial and temporal variations of ARF over the vast territory of China for the first time using observational data, as described in this paper.

2. Data and Methodology

[6] Ground-based measurements from the Chinese Sun Hazemeter Network (CSHNET), established under the

[1]ESSIC, Department of Atmospheric and Oceanic Science, University of Maryland, College Park, Maryland, USA.
[2]Institute of Atmospheric Physics, Chinese Academy of Sciences, Beijing, China.
[3]School of Atmospheric Physics, Nanjing University of Information Science and Technology, Nanjing, China.
[4]Department of Satellite Geoinformatics Engineering, Kyungil University, Geongsan, South Korea.
[5]RMRS Fire Sciences Laboratory, U.S. Forest Service, Missoula, Montana, USA.

0148-0227/10/2009JD013306

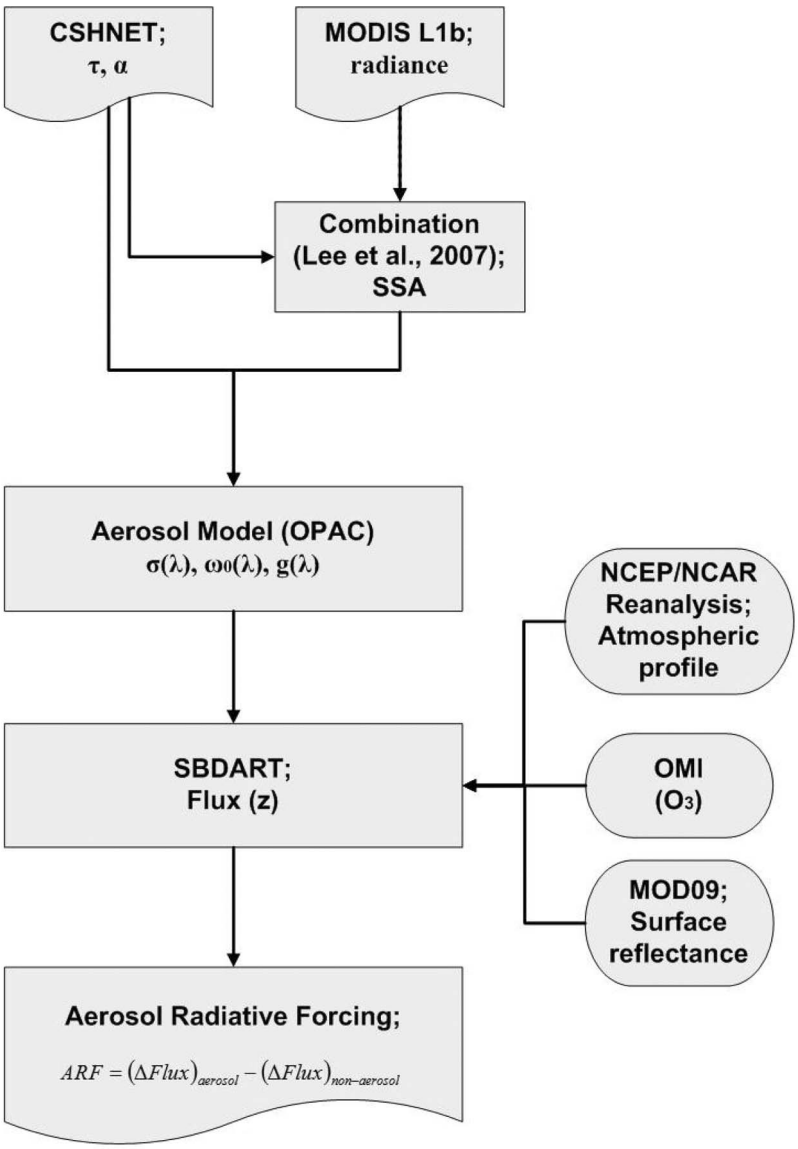

Figure 1. Schematic diagram of the approach taken in this study to calculate aerosol radiative forcing (ARF) and atmospheric heating rates. Both ground-based and satellite observation data were used in SBDART to calculate fluxes.

auspices of the EAST-AIRE, were used to retrieve aerosol optical properties. Since August 2004, the CSHNET has provided continuous measurements of spectral aerosol optical thickness (AOT) and Ångström exponent (AE) at 25 stations across China [*Xin et al.*, 2007; *Wang et al.*, 2008]. Together with reflectance measured by the Moderate Resolution Imaging Spectroradiometer (MODIS) satellite sensor at the top-of-atmosphere (TOA), SSA was estimated at these sites [*Lee et al.*, 2007]. Both data sets are used in this study to estimate ARF. To account for the spectral dependence of aerosol properties, different combinations of the aerosol models of *Hess et al.* [1998] were matched with the AE and SSA data. The combination of aerosol models that match most closely with AE and SSA data is used. The method is evaluated using Aerosol Robotic Network (AERONET) retrieved aerosol spectral properties at four of the 25 CSHNET stations in China (Beijing, 116.381°E, 39.977°N; Hefei, 117.162°E, 31.905°N; Taihu, 120.215°E, 31.421°N; Xianghe, 116.962°E, 39.754°N).

[7] Other data sets used in the study include ozone concentrations from the Ozone Monitoring Instrument (OMI), atmospheric profiles from the National Centers for Environmental Prediction and the National Center for Atmospheric Research reanalysis project [*Kalnay et al.*, 1996], and surface reflectances from the 500 m resolution MODIS Level 2 Collection 5 spectral surface reflectance product (MOD09). The Santa Barbara DISORT Atmospheric Radiative Transfer (SBDART) [*Ricchiazzi et al.*, 1998] code is used to perform radiative transfer calculations in the shortwave (SW) spectral region (0.25–4.0 μm). ARF is determined as the difference in net flux with and without aerosols under cloud-free conditions. The same atmospheric and environmental variables (water vapor, ozone, surface albedo, etc.) are used as input to the SBDART

Table 1. Uncertainty of Input Parameters for SBDART Calculations and the Resulting Errors in Computed Fluxes[a]

Parameters	Uncertainty	Input Range	Error (W m^{-2})
AOT	2–6%[b]	±0.02	2.24 ± 0.91
Ångström exponent	NA	±0.1	NA
SSA	~0.03[c]	±0.03	8.79 ± 2.98
Asymmetry parameter	NA	±0.03	2.28 ± 1.28
Surface reflectance	±(0.005+5%)[d]	±0.01	3.43 ± 1.93
Ozone	2%[e]	±10	0.17 ± 0.04
Relative humidity	NA	±10%	NA
Combined	NA	NA	8.76 ± 3.44

[a]NA; not available.
[b]*Xin et al.* [2007].
[c]*Lee et al.* [2007].
[d]*Vermote and Kotchenova* [2008].
[e]*Veefkind et al.* [2006].

model for both aerosol and aerosol-free simulations. Measured AOT data are used to determine fluxes in the presence of aerosols. The methodology used in this study is illustrated in Figure 1.

[8] The uncertainties of the input parameters (as specified in Table 1) are based on previous studies [*Xin et al.*, 2007; *Lee et al.*, 2007; *Vermote and Kotchenova*, 2008; *Veefkind et al.*, 2006]. The resulting errors in the estimates of ARF are estimated on the basis of the uncertainty ranges of input variables such as AOT, Ångström exponent, SSA, surface albedo, ozone, and relative humidity. A sensitivity study was performed to determine the error in ARF incurred by an error in each of the input parameters for SBDART. The error is the difference between the flux calculated with and without the error in the parameter under study against that calculated for the following controlled values: AOT_{550} = 0.69, $AE_{470–660}$ = 1.06, SSA_{550} = 0.89, and broadband surface albedo is 0.3.

[9] Because of the large uncertainty in SSA [*Lee et al.*, 2007] and the generally heavy aerosol loading in the region, SSA is the largest source of error in calculating ARF. This is because aerosol absorption affects the radiation budgets at all three levels of the atmosphere. Generally, the uncertainty in the flux calculation from the SSA retrieval is as much as 8.79 ± 2.98 W m^{-2}. By comparing AOT derived from CSHNET and CIMEL Sun photometers operating at the same locations in China, *Xin et al.* [2007] estimated a relative error of 2% ~ 6% for AOT, which transforms into an error of 2.24 ± 0.91 W m^{-2} in the calculation of surface fluxes.

[10] The error caused by surface reflectance is also important in radiative transfer calculations. The accuracy in MODIS land surface reflectance (±0.01) reported by *Vermote and Kotchenova* [2008] is used in the error analysis. The resulting error by surface reflectance is typically small in the downward direction but large in the upward direction. The mean error is substantially smaller (3.43 ± 1.93 W m^{-2}) than that due to SSA but larger than the error due to AOT. Uncertainty of the OMI ozone data is reported as 2% [*Veefkind et al.*, 2006]. We used ±10 ppb as the uncertainty for ozone concentration in the error analysis. The resulting error by ozone is quite small, with a mean value of 0.17 ± 0.04 W m^{-2}.

[11] The overall errors are obtained by assuming that individual errors are independent of each other. The errors

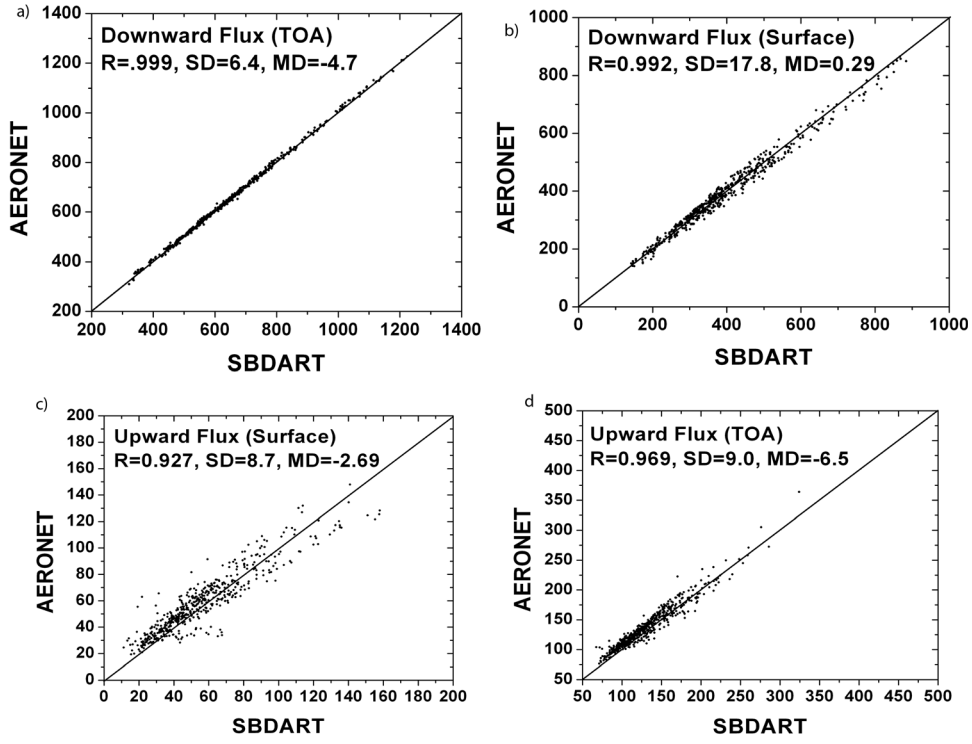

Figure 2. Upward and downward SW fluxes at the surface and TOA from the AERONET inversion product as a function of upward and downward SW fluxes at the surface and TOA from SBDART calculations.

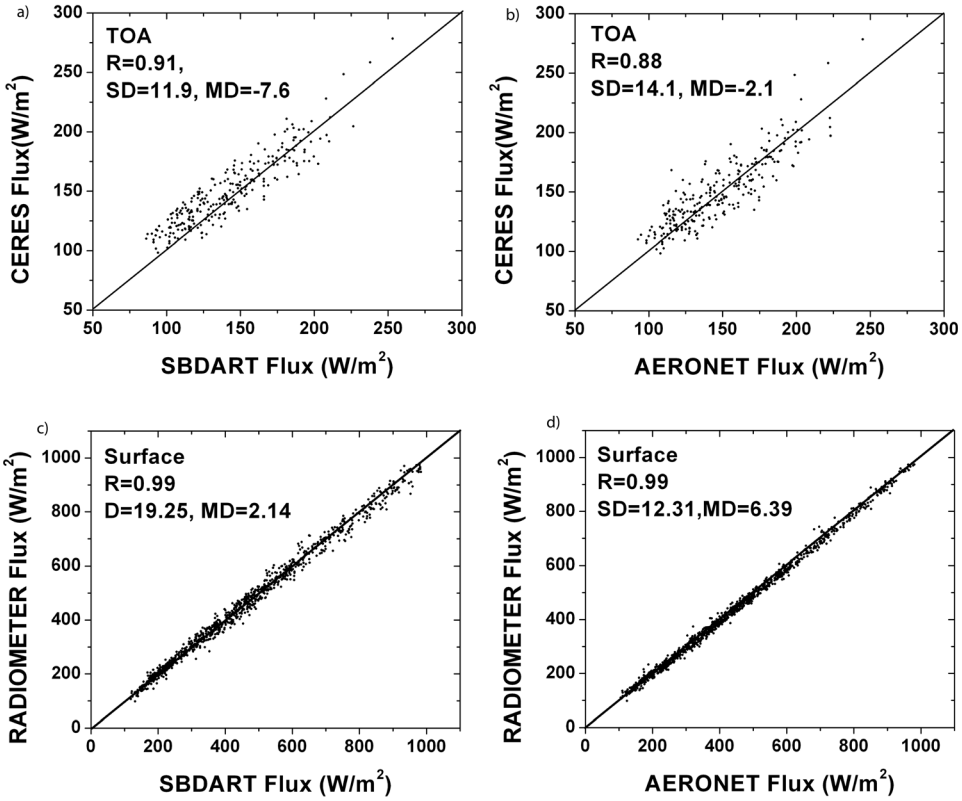

Figure 3. Upward SW fluxes at the TOA from CERES observations as a function of upward SW fluxes from the (a) AERONET inversion product and (b) SBDART calculations and (c) downward SW fluxes at the surface measured by broadband radiometers as a function of SBDART calculations and (d) from the AERONET inversion product.

were computed using the following values: (1) AOT = 0.67, 0.69, and 0.71, (2) SSA = 0.86, 0.89, and 0.91, (3) asymmetry parameters of±0.03, (4) surface reflectance of 0.29, 0.30, and 0.31, and (5) ozone amounts of 350, 360, and 370 Dobson units. The overall errors are largest in downward fluxes at the surface (10.84 ± 2.82 W m^{-2}) and smallest in upward fluxes at the surface (6.62 ± 2.43 W m^{-2}). The error in upward fluxes at the TOA is 7.81 ± 2.11 W m^{-2}. Note that the combined error in the flux calculations is 8.76 ± 3.44 W m^{-2}.

3. Evaluation of the Method by Comparisons to Independent Data Sets

[12] As a check of the aerosol spectral optical properties derived from matching with the database developed by *Hess et al.* [1998] as described above, surface and TOA radiative fluxes calculated using SBDART are compared to the aerosol products derived from AERONET CIMEL Sun photometers. In addition to more channels, AERONET CIMEL retrievals have more output variables than those derived from the CSHNET. However, there are fewer AERONET stations located in China. Level 2.0 AERONET aerosol products [*Smirnov et al.*, 2006] are inverted from sky radiance and direct beam measurements at four wavelengths (440, 670, 870, 1020 nm) [*Dubovik et al.*, 2000]. The products include both aerosol physical parameters (i.e., size distribution and complex refractive index) and optical properties (e.g., phase function, single-scattering albedo, spectral and broadband fluxes).

[13] Figure 2 shows comparisons of downward and upward fluxes at the surface and TOA from AERONET retrievals and SBDART calculations. In general, the correlations between fluxes calculated with the two sets of data are very good. The correlation coefficients, mean differences, and standard deviations range from 0.927 to 0.999, from 0.29 to 6.5, and from 6.4 to 17.8 W m^{-2}, respectively. The relative differences are generally less than 5% for downward fluxes and 10% for upward fluxes.

[14] The above numbers do not denote real uncertainties incurred in our calculations because AERONET aerosol products are inferred rather than measured. Direct observation data from Xianghe are thus used to evaluate SBDART results. Upward TOA fluxes from Terra's Clouds and Earth's Radiant Energy System (CERES) satellite measurements (0.3–4 μm) and surface downward fluxes from broadband radiometers (Kipp and Zonen's CM11 and CM21 models, λ = 0.3–3 μm) are compared to model calculations. At the Xianghe site, AERONET and CSHNET aerosol data are available, so two sets of TOA upwelling and surface downwelling fluxes are computed using SBDART. Both sets of modeled flux data are compared to TOA and surface measurements. CERES satellite data within 50 km of the Xianghe site were matched with ground measurements of aerosols and fluxes acquired within ±30 min of the CERES overpass time. CERES measures radiances that are

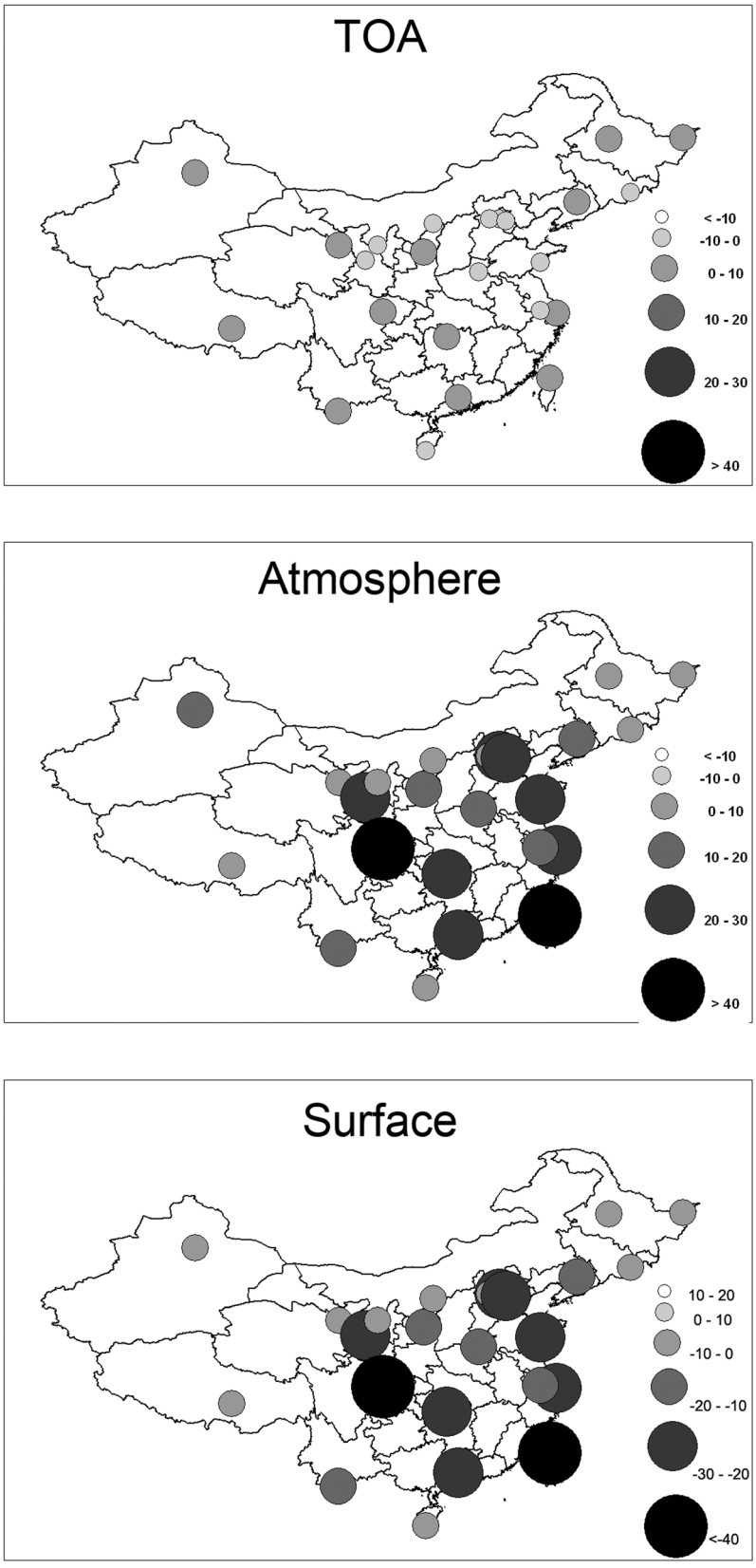

Figure 4. Annual mean SW aerosol radiative forcing from 2005.

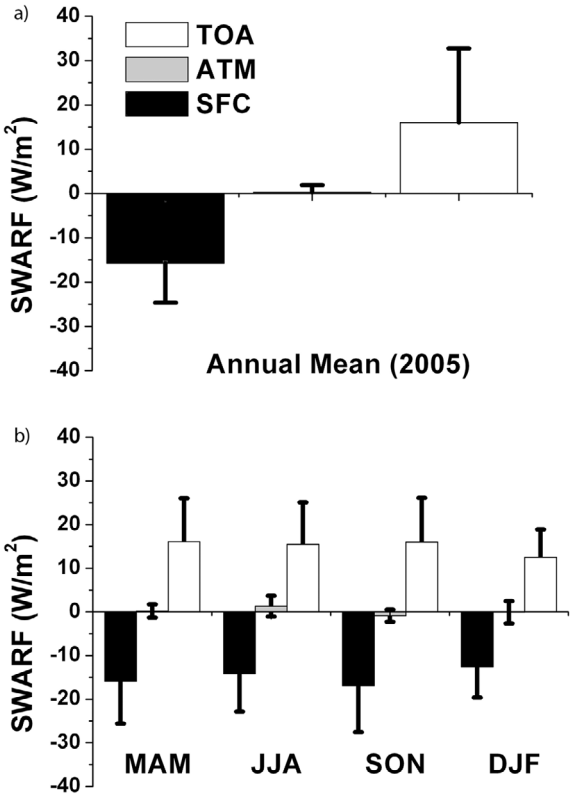

Figure 5. (a) Mean annual and (b) seasonal shortwave aerosol radiative forcing (SWARF) over China.

converted to broadband fluxes using angular distribution models. Uncertainties in SW CERES fluxes are estimated to be within 13 W m^{-2} for all-sky conditions and somewhat less for clear-sky cases [*Chambers et al.*, 2001; *Loeb et al.*, 2003a; 2003b]. Uncertainties in SW broadband fluxes from the radiometers are less than 2% (<10 W m^{-2}) according to the manufacturer's specifications.

[15] The comparison results are presented in Figure 3. The agreements at the surface are exceptionally good for both sets of computed fluxes in comparison with radiometer measurements. Their standard deviations are 19.25 and 12.31 W m^{-2}, and their mean differences are 2.14 and 6.39 W m^{-2} for CSHNET and AERONET, respectively. The agreement for TOA fluxes is worse in terms of relative difference but compatible in terms of absolute difference. A mismatch in the spatial coverage between satellite and ground-based measurements is the primary cause for the large relative difference as demonstrated by *Li et al.* [1995].

4. Results

[16] Shortwave aerosol radiative forcing (SWARF or F) depends highly on aerosol loading and optical properties, the intensity of incoming solar energy, and the surface albedo. Diurnal mean SWARF (dF) is often expressed as

$$dF = \frac{1}{24\text{h}} \int F(t)dt, \tag{1}$$

where $F(t)$ denotes instantaneous SWARF values under clear-sky conditions computed from observed AOT and

Table 2. Summary of Forcing Efficiency f_e Over China During EAST-AIRE 2005 and From Other Studies[a]

Aerosol Type	SSA	f_e^{SFC}	f_e^{TOA}	f_e^{ATM}	Campaign	Location	Date	Sources
Anthropogenic, dust	0.89	−227.1 ± 38.10	−2.1 ± 23.37	224.99 ± 50.0	EAST-AIRE	China	2005	This study
Anthropogenic, dust	0.874 ± 0.028	−202.2 ± 40.4	NA	NA	INDOEX	KCO, Maldives	Feb–Mar 1999	*Bush and Valero* [2002]
Anthropogenic, dust	NA	−173.0 ± 32.9	NA	NA	ACE-Asia	Gosan, Korea	Mar–May 2001	*Bush and Valero* [2003]
Anthropogenic, dust	~0.8	−116.9	−15.3	102	NA	Korea	Apr 2000	*Costa et al.* [2006]
Anthropogenic	0.85 ± 0.07	−116.06	−19.79	96.27	NA	southeast United States, 1995	Jun–Dec 1995	*Yu et al.* [2001]
Anthropogenic	~0.92	−150	NA	NA	ADRIEX	Venice, Italy	Aug–Sep 2004	*Barnaba et al.* [2007]
Biomass burning	~0.91	NA	−22.8	NA	NA	Southeast Asia	Oct 1997	*von Hoyningen-Huene et al.* [1999]
Biomass burning	0.865	−101	−34	67	SAFARI	South Africa	Sep 2000	*Ichoku et al.* [2003]
Saharan dust	~0.97	NA	−50.68	NA	NA	Atlantic	Jul 1998	*Liu et al.* [2004]

[a]NA; not available.

Table 3. Diurnal Aerosol Radiative Forcing Efficiency df_e at the Ground Measurement Sites[a]

Site	df_e^{SFC}	df_e^{TOA}	df_e^{ATM}
Ansai	−31.8 ± 2.3(0.69)	−1.2 ± 0.8(0.02)	33.1 ± 1.9(0.80)
Beijing	−61.2 ± 3.5(0.88)	−6.6 ± 1.4(0.62)	54.6 ± 4.1(0.79)
Beijing Forest	−29.2 ± 2.4(0.69)	−3.5 ± 1.2(0.31)	25.6 ± 2.6(0.63)
Changbai Mt.	−35.1 ± 2.5(0.65)	NS	35.9 ± 1.7(0.87)
Dinghu Mt.	−37.6 ± 1.6(0.94)	0.43 ± 1.5(0.03)	38.0 ± 0.6(0.99)
Eerduosi	−25.1 ± 1.7(0.45)	NS	25.1 ± 1.5(0.40)
Fengqiu	−24.3 ± 1.5(0.67)	−0.2 ± 0.8(0.2)	24.1 ± 1.5(0.68)
Fukang	−22.3 ± 1.8(0.75)	7.8 ± 2.1(0.84)	30.0 ± 0.9(0.98)
Haibei	NS	NS	23.8 ± 1.9(0.69)
Hailun	−32.3 ± 1.8(0.64)	NS	33.6 ± 2.3(0.79)
Jiaozhouwan	−36.0 ± 1.0(0.97)	−4.2 ± 0.5(0.21)	31.8 ± 1.0(0.98)
Lanzhou	−32.3 ± 2.1(0.80)	NS	31.8 ± 2.7(0.63)
Lasha	−30.6 ± 1.0(0.84)	NS	34.5 ± 1.8(0.87)
Sanjiang	−36.4 ± 4.3(0.63)	4.9 ± 3.0(0.67)	41.3 ± 3.6(0.45)
Sanya	−46.0 ± 1.8(0.97)	−2.9 ± 0.9(0.15)	43.2 ± 3.0(0.95)
Shanghai	−37.9 ± 1.6(0.89)	NS	39.2 ± 2.0(0.91)
Shapotou	−20.7 ± 1.5(0.06)	NS	20.6 ± 1.9(0.02)
Shenyang	−31.7 ± 1.8(0.85)	NS	35.1 ± 1.4(0.95)
Taihu	−32.9 ± 3.1(0.63)	−5.5 ± 0.6(0.34)	27.4 ± 3.1(0.61)
Taoyuan	NS	0.5 ± 1.0(0.31)	28.5 ± 2.3(0.28)
Xianghe	−65.4 ± 4.7(0.65)	−2.9 ± 1.9(0.53)	62.5 ± 3.7(0.79)
Yanting	−32.9 ± 2.8(0.57)	1.4 ± 1.7(0.06)	34.2 ± 3.1(0.50)
Xishuangbanna	−35.62(0.94)	4.7 ± 1.5(0.02)	40.3 ± 2.5(0.90)
Taibei	NS	NS	NS
Average	−35.1	−0.5	34.5

[a]Correlation coefficients from linear fitting are given in parentheses. NS; not significant.

estimated aerosol optical properties as explained above. On an individual day, the number of data points is limited because of the presence of clouds. To overcome this limitation, monthly mean values at 25 discrete time intervals were determined from which monthly and annual means of SWARF are computed.

[17] Figure 4 shows the annual mean SWARF estimated under clear skies during 2005. The operation of 25 CSHNET stations provides an opportunity to display the spatial variation of aerosols and their radiative forcing, although some regions such as the northwest are poorly sampled. Satellite and ground-based observations reveal that most anthropogenic aerosol sources are located in the highly populated eastern region of China [*Li et al.*, 2007a; 2007c] and that natural dust storms mainly originate from the desert region in the northwest [*Xu et al.*, 2004]. In general, the magnitudes of surface and atmospheric SWARF are very large but of opposite signs. The largest negative F_{SFC} (−20 to −32 W m^{-2}) and positive F_{ATM} (20–40 W m^{-2}) were found over east China, implying strongest cooling at the surface and warming in the atmosphere. They are induced by large AOT and small SSA [e.g., *Zhao and Li*, 2007; *Lee et al.*, 2007]. Owing to the trade-off between the two large but virtually identical SWARFs at the surface and within the atmosphere, TOA SWARF (F_{TOA}) is very small. The mean values of surface SWARF (F_{SFC}), atmosphere SWARF (F_{ATM}), and F_{TOA} for all CSHNET stations are shown in Figure 5a and are equal to −15.7 ± 9.0, 16.0 ± 9.2, and 0.3 ± 1.6 W m^{-2}, respectively. Note that standard deviations in Figure 5a do not represent errors but spatiotemporal variability. To put this in perspective, the global mean values obtained over the global continents from observations are −11.9, 7.0, and −4.9 W m^{-2}, respectively, and by modeling are −7.6, 4.0, and −3.0 W m^{-2}, respectively

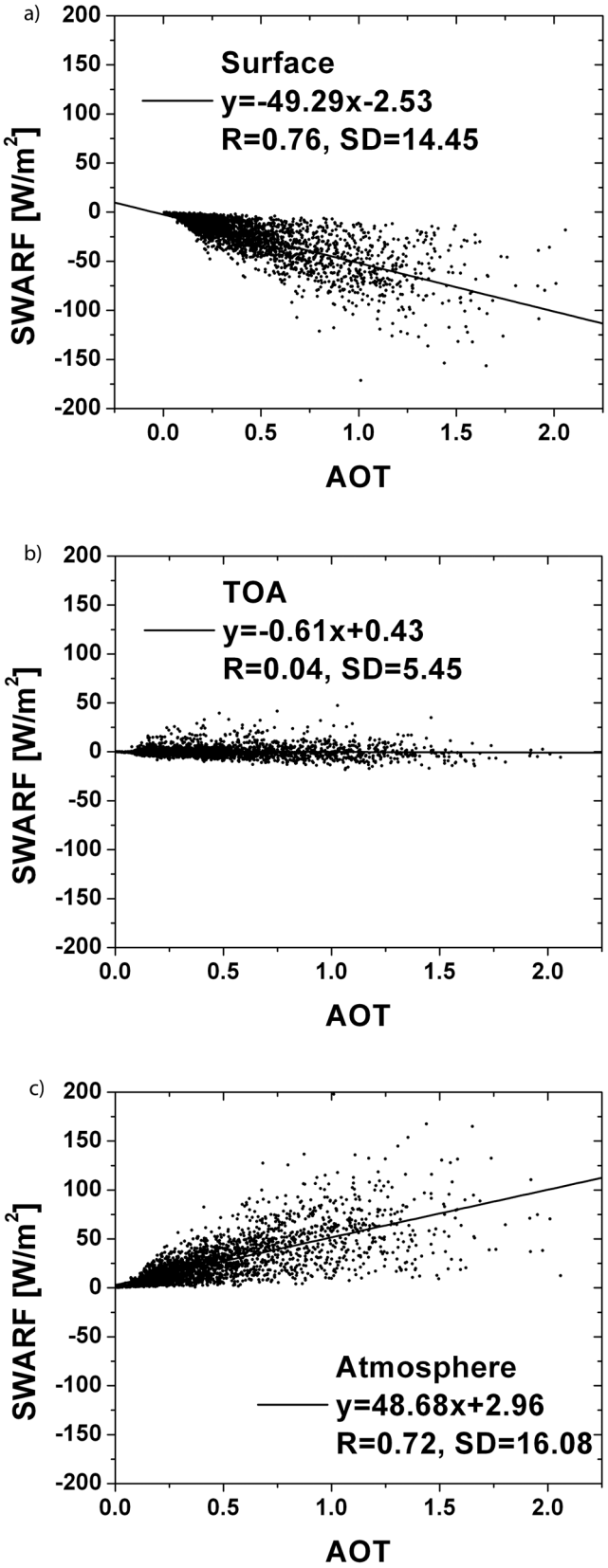

Figure 6. Diurnal aerosol radiative forcing at the TOA within the atmosphere and at the surface as a function of AOT over the study area.

[*Yu et al.*, 2006, 2009]. F_{ATM} is similar to the regional mean value. The largest negative F_{SFC} ($-32 \sim -20$ W m^{-2}) and positive F_{ATM} ($40 \sim 20$ W m^{-2}) were found over east China, implying strongest cooling at the surface and warming in the atmosphere. They are induced by large AOT and small SSA [e.g., *Zhao and Li*, 2007; *Lee et al.*, 2007]. Figure 5b illustrates the seasonal variation in aerosol forcing. F_{ATM} in China can reach 16 W m^{-2} during the summer and autumn seasons. All three forcing values, F_{SFC}, F_{ATM}, and F_{TOA}, have maximum values during the summer and minimum values during the winter.

[18] The diurnal mean SWARF forcing efficiency over China and from other regions around the world is summarized in Table 2. The magnitude of surface forcing in China is larger than the global mean but still less than those found during ACE-Asia and Transport and Chemical Evolution over the Pacific (TRACE-P) [*Bates et al.*, 2006], the Aerosol Direct Radiative Impact Experiment (ADRIEX) [*Barnaba et al.*, 2007], the United Arab Emirates (UAE), Unified Aerosol Experiment (UAE^2) [*Markowicz et al.*, 2008], and ground-based sky radiometer network (SKYNET) measurements in East Asia [*Kim et al.*, 2005]. This is partially due to the fact that the region of our study is larger than the domains of most experimental studies which mainly focused on areas with heavy aerosol loading. However, the forcing in the atmosphere across China is larger than those found in most other places, suggesting stronger absorbing aerosols present in the region. As a result, it is not surprising to see much smaller TOA forcing over China than at most other places listed in Table 2.

[19] Aerosol radiative forcing efficiencies, defined as forcing per unit AOT, at the ground measurement sites are given in Table 3. Mean values over China are -0.5 at the TOA, 34.5 within the atmosphere, and -35.1 W m^{-2} τ^{-1} at the surface. The largest magnitudes of forcing at the surface are found in Xianghe (-65.4 ± 4.7 W m^{-2} τ^{-1}) and Beijing (-61.2 ± 3.5 W m^{-2} τ^{-1}). These values are slightly less than those calculated from the INDOEX (-72.2 ± 5.5 W m^{-2} τ^{-1}) and those over the ACE-Asia domain (-73.0 ± 9.6 W m^{-2} τ^{-1}) but are still comparable. Figure 6 plots diurnal aerosol radiative forcing efficiency at the surface (df_e^{SFC}), atmosphere (df_e^{ATM}), and TOA (df_e^{TOA}) as a function of AOT. The slope of the linear fitting line represents the mean df_e over China. The large scattering in the data points implies that aerosol composition varies greatly over the domain covered by the observation sites during the period of study, which is partly due to variable aerosol SSA [*Lee et al.*, 2007].

5. Conclusion

[20] Aerosol radiative forcing (ARF) is a measure of the impact of human and natural processes on the climate system. Using an extensive set of aerosol observational data as input to a radiative transfer model, we attempt to derive the first observation-based estimate of ARF across China. Model input data include aerosol optical depth measurements made at 25 stations distributed across China, single-scattering albedos estimated from a combination of satellite and ground measurements, surface albedo data retrieved from the satellite-borne MODIS, and ozone data from Total Ozone Mapping Spectrometer (TOMS). Aerosol radiative forcing is computed at the top, bottom, and interior of the atmosphere. Nationwide diurnal mean aerosol forcings are 15.7 ± 9.0 at the surface, 0.3 ± 1.6 at the TOA, and 16.0 ± 9.2 W m^{-2} inside the atmospheric column. The near balanced SWARF for the atmosphere-surface system indicates the presence of strong absorbing aerosols across the region which almost entirely offsets the effect of aerosol scattering. The huge amount of solar radiation trapped inside the atmosphere by aerosols is a significant source of heating to the atmosphere, especially within the lower atmosphere. This can substantially alter atmospheric stability and influence the dynamic system. The validity of the method is demonstrated using independent ground and satellite observations. Uncertainties of our estimates are also quantified.

[21] **Acknowledgments.** The study was supported by funding from the MOST (2006CB403706), NASA (NNX08AH71G), and DOE (DEFG0208ER64571).

References

Barnaba, F., G. P. Gobbi, and G. de Leeuw (2007), Aerosol stratification, optical properties and radiative forcing in Venice (Italy) during ADRIEX, *Q. J. R. Meteorol. Soc.*, *133*(S1), 47–60, doi:10.1002/qj.91.

Bates, T. S., et al. (2006), Aerosol direct radiative effects over the northwest Atlantic, northwest Pacific, and north Indian oceans: Estimates based on in-situ chemical and optical measurements and chemical transport modeling, *Atmos. Chem. Phys.*, *6*, 1657–1732, doi:10.5194/acp-6-1657-2006.

Bush, B. C., and F. P. J. Valero (2002), Spectral aerosol radiative forcing at the surface during the Indian Ocean Experiment (INDOEX), *J. Geophys. Res.*, *107*(D19), 8003, doi:10.1029/2000JD000020.

Bush, B. C., and F. P. J. Valero (2003), Surface aerosol radiative forcing at Gosan during the ACE-Asia campaign, *J. Geophys. Res.*, *108*(D23), 8660, doi:10.1029/2002JD003233.

Chambers, L. H., B. A. Wielicki, and N. G. Loeb (2001), Shortwave flux from satellite-measured radiance: A theoretical study over marine boundary layer clouds, *J. Appl. Meteorol.*, *40*, 2144–2161, doi:10.1175/1520-0450(2001)040<2144:SFFSMR>2.0.CO;2.

Charlson, R. J., S. E. Schwartz, J. H. Hales, R. D. Cess, J. A. Coakley Jr., J. E. Hansen, and D. J. Hofmann (1992), Climate forcing by anthropogenic aerosols, *Science*, *255*, 423–430, doi:10.1126/science.255.5043.423.

Costa, M. J., B. J. Sohn, V. Levizzani, and A. M. Silva (2006), Radiative forcing of Asian dust determined from the synergized GOME and GMS satellite data—A case study, *J. Meteorol. Soc. Jpn.*, *84*, 85–95, doi:10.2151/jmsj.84.85.

Dubovik, O., S. Smirnov, B. N. Holben, M. D. King, Y. J. Kaufman, T. F. Eck, and I. Slutsker (2000), Accuracy assessments of aerosol optical properties retrieved from Aerosol Robotic Network AERONET Sun and sky radiance measurements, *J. Geophys. Res.*, *105*(D8), 9791–9806, doi:10.1029/2000JD900040.

Hansen, J., M. Sato, R. Ruedy, A. Lacis, and V. Oinas (2000), Global warming in the twenty-first century: An alternative scenario, *Proc. Natl. Acad. Sci. U. S. A.*, *97*(18), 9875–9880, doi:10.1073/pnas.170278997.

Hess, M., P. Koepke, and I. Schultz (1998), Optical properties of aerosols and clouds: The software package OPAC, *Bull. Am. Meteorol. Soc.*, *79*, 831–844, doi:10.1175/1520-0477(1998)079<0831:OPOAAC>2.0.CO;2.

Huebert, B. J., T. Bates, P. B. Russell, G. Shi, Y. J. Kim, K. Kawamura, G. Carmichael, and T. Nakajima (2003), An overview of ACE-Asia: Strategies for quantifying the relationships between Asian aerosols and their climatic impacts, *J. Geophys. Res.*, *108*(D23), 8633, doi:10.1029/2003JD003550.

Ichoku, C., L. A. Remer, Y. J. Kaufman, R. Levy, D. A. Chu, D. Tanré, and B. N. Holben (2003), MODIS observation of aerosols and estimation of aerosol radiative forcing over southern Africa during SAFARI 2000, *J. Geophys. Res.*, *108*(D13), 8499, doi:10.1029/2002JD002366.

Intergovernmental Panel on Climate Change (2007), *Climate Change 2007: The Scientific Basis. Contribution of Working Group I to the Fourth Assessment Report of the Intergovernmental Panel on Climate Change*, edited by S. Solomon et al., Cambridge Univ. Press, New York.

Jacobson, M. Z. (2001), Strong radiative heating due to the mixing state of black carbon in atmospheric aerosols, *Nature*, *409*, 695–697, doi:10.1038/35055518.

Kalnay, E., et al. (1996), The NCEP/NCAR 40-year reanalysis project, *Bull. Am. Meteorol. Soc.*, *77*, 437–471, doi:10.1175/1520-0477(1996)077<0437:TNYRP>2.0.CO;2.

Kaufman, Y. J., I. Koren, L. A. Remer, D. Rosenfeld, and Y. Rudich (2005), The effect of smoke, dust, and pollution aerosol on shallow cloud development over the Atlantic Ocean, *Proc. Natl. Acad. Sci. U. S. A.*, *102*(32), 11,207–11,212, doi:10.1073/pnas.0505191102.

Kim, D.-H., B. J. Sohn, T. Nakajima, and T. Takamura (2005), Aerosol radiative forcing over east Asia determined from ground-based solar radiation measurements, *J. Geophys. Res.*, *110*, D10S22, doi:10.1029/2004JD004678.

Lee, K. H., Z. Li, M. S. Wong, J. Xin, Y. Wang, W.-M. Hao, and F. Zhao (2007), Aerosol single-scattering albedo estimated across China from a combination of ground and satellite measurements, *J. Geophys. Res.*, *112*, D22S15, doi:10.1029/2007JD009077.

Li, Z. (1998), Influence of absorbing aerosols on the inference of solar surface radiation budget and cloud absorption, *J. Clim.*, *11*, 5–17, doi:10.1175/1520-0442(1998)011<0005:IOAAOT>2.0.CO;2.

Li, Z., T. Charlock, and C. Whitlock (1995), Assessment of the global monthly mean surface insolation estimated from satellite measurements using global energy balance archive data, *J. Clim.*, *8*, 315–328, doi:10.1175/1520-0442(1995)008<0315:AOTGMM>2.0.CO;2.

Li, Z., et al. (2007a), Preface to special section on East Asian Studies of Tropospheric Aerosols: An International Regional Experiment (EAST-AIRE), *J. Geophys. Res.*, *112*, D22S00, doi:10.1029/2007JD008853.

Li, Z., et al. (2007b), Aerosol optical properties and their radiative effects in northern China, *J. Geophys. Res.*, *112*, D22S01, doi:10.1029/2006JD007382.

Li, Z., F. Niu, K.-H. Lee, J. Xin, W.-M. Hao, B. Nordgren, Y. Wang, and P. Wang (2007c), Validation and understanding of Moderate Resolution Imaging Spectroradiometer aerosol products (C5) using ground-based measurements from the handheld Sun photometer network in China, *J. Geophys. Res.*, *112*, D22S07, doi:10.1029/2007JD008479.

Liu, X., J. Wang, and S. A. Christopher (2004), Shortwave direct radiative forcing of Saharan dust aerosols over the Atlantic Ocean, *Int. J. Remote Sens.*, *24*, 5147–5160, doi:10.1080/0143116031000114824.

Loeb, N. G., et al. (2003a), Angular distribution models for top-of-atmosphere radiative flux estimation from the Clouds and the Earth's Radiant Energy System instrument on the Tropical Rainfall Measuring Mission satellite. Part I: Methodology, *J. Appl. Meteorol.*, *42*, 240–265, doi:10.1175/1520-0450(2003)042<0240:ADMFTO>2.0.CO;2.

Loeb, N. G., et al. (2003b), Angular distribution models for top-of-atmosphere radiative flux estimation from the Clouds and the Earth's Radiant Energy System instrument on the Tropical Rainfall Measuring Mission satellite. Part II: Validation, *J. Appl. Meteorol.*, *42*, 1748–1769, doi:10.1175/1520-0450(2003)042<1748:ADMFTR>2.0.CO;2.

Markowicz, K. M., P. J. Flatau, J. Remiszewska, M. Witek, E. A. Reid, J. S. Reid, A. Bucholtz, and B. Holben (2008), Observations and modeling of the surface aerosol radiative forcing during the UAE^2 experiment, *J. Atmos. Sci.*, *65*, 2877–2891, doi:10.1175/2007JAS2555.1.

Menon, S., J. Hansen, L. Nazarenko, and Y. Luo (2002), Climate effects of black carbon aerosols in China and India, *Science*, *297*, 2250–2253, doi:10.1126/science.1075159.

Nakajima, T., et al. (2003), Significance of direct and indirect radiative forcings of aerosols in the East China Sea region, *J. Geophys. Res.*, *108* (D23), 8658, doi:10.1029/2002JD003261.

Ramanathan, V., P. J. Crutzen, J. T. Kiehl, and D. Rosenfeld (2001a), Aerosol, climate, and hydrological cycle, *Science*, *294*, 2119–2124, doi:10.1126/science.1064034.

Ramanathan, V., et al. (2001b), Indian Ocean Experiment: An integrated analysis of the climate forcing and effects of the great Indo-Asian haze, *J. Geophys. Res.*, *106*, 28,371–28,398, doi:10.1029/2001JD900133.

Ramanathan, V., et al. (2007), Atmospheric brown clouds: Hemispherical and regional variations in long-range transport, absorption, and radiative forcing, *J. Geophys. Res.*, *112*, D22S21, doi:10.1029/2006JD008124.

Ricchiazzi, P., S. Yang, C. Gautier, and D. Sowle (1998), SBDART: A research and teaching tool for plane-parallel radiative transfer in the Earth's atmosphere, *Bull. Am. Meteorol. Soc.*, *79*, 2101–2114, doi:10.1175/1520-0477(1998)079<2101:SARATS>2.0.CO;2.

Smirnov, A., et al. (2006), Ship-based aerosol optical depth measurements in the Atlantic Ocean: Comparison with satellite retrievals and GOCART model, *Geophys. Res. Lett.*, *33*, L14817, doi:10.1029/2006GL026051.

Veefkind, J. P., J. F. de Haan, E. J. Brinksma, M. Kroon, and P. F. Levelt (2006), Total ozone from the Ozone Monitoring Instrument (OMI) using the DOAS technique, *IEEE Trans. Geosci. Remote Sens.*, *44*(5), 1239–1244, doi:10.1109/TGRS.2006.871204.

Vermote, E. F., and S. Y. Kotchenova (2008), MOD09 (surface reflectance) user's guide, version 1.1, *MODIS Land Surface Reflectance Sci. Comput. Facil.*, College Park, Md., March.

von Hoyningen-Huene, W., T. Schmidt, S. Schienbein, C. A. Kee, and L. J. Tick (1999), Climate-relevant aerosol parameters of south-east-Asian forest fire haze, *Atmos. Environ.*, *33*(19), 3183–3190, doi:10.1016/S1352-2310(98)00422-1.

Wang, Y., et al. (2008), Seasonal variations in aerosol optical properties over China, *Atmos. Chem. Phys. Discuss.*, *8*, 8431–8453, doi:10.5194/acpd-8-8431-2008.

Xia, X., Z. Li, B. Holben, P. Wang, T. Eck, H. Chen, M. Cribb, and Y. Zhao (2007), Aerosol optical properties and radiative effects in the Yangtze Delta region of China, *J. Geophys. Res.*, *112*, D22S12, doi:10.1029/2007JD008859.

Xin, J., et al. (2007), Aerosol optical depth (AOD) and Ångström exponent of aerosols observed by the Chinese Sun Hazemeter Network from August 2004 to September 2005, *J. Geophys. Res.*, *112*, D05203, doi:10.1029/2006JD007075.

Xu, J., M. H. Bergin, R. Greenwald, J. J. Schauer, M. M. Shafer, J. L. Jaffrezo, and G. Aymoz (2004), Aerosol chemical, physical, and radiative characteristics near a desert source region of northwest China during ACE-Asia, *J. Geophys. Res.*, *109*, D19S03, doi:10.1029/2003JD004239.

Yu, H., et al. (2006), A review of measurement-based assessments of aerosol direct radiative effect and forcing, *Atmos. Chem. Phys.*, *6*, 613–666, doi:10.5194/acp-6-613-2006.

Yu, H., et al. (2009), Remote sensing and in-situ measurements of aerosol properties, burdens, and radiative forcing, in *Atmospheric Aerosol Properties and Climate Impacts: Synthesis and Assessment Product 2.3: Report by the U.S. Climate Change Science Program and the Subcommittee on Global Change Research*, edited by M. Chi, R. A. Kahn, and S. E. Schwartz, pp. 21–54, U.S. Clim. Change Sci. Program, Washington, D. C.

Yu, S., C. S. Zender, and V. K. Saxena (2001), Direct radiative forcing and atmospheric absorption by boundary layer aerosol in the southeastern US: Model estimates on the basis of new observations, *Atmos. Environ.*, *35*(23), 3967–3977, doi:10.1016/S1352-2310(01)00187-X.

Zhao, F., and Z. Li (2007), Estimation of aerosol single-scattering albedo from solar direct spectral radiance and total broadband irradiances measured in China, *J. Geophys. Res.*, *112*, D22S03, doi:10.1029/2006JD007384.

W.-M. Hao, RMRS Fire Sciences Laboratory, U.S. Forest Service, 5775 W. U.S. Hwy. 10, Missoula, MT 59808, USA.

K.-H. Lee, Department of Satellite Geoinformatics Engineering, Kyungil University, Geongsan, Gyeongsangbuk-do 712-701, South Korea.

Z. Li, ESSIC, Department of Atmospheric and Oceanic Science, University of Maryland, College Park, MD 20740, USA. (zli@atmos.umd.edu)

Y. Wang and J. Xin, Institute of Atmospheric Physics, Chinese Academy of Sciences, Beijing 100083, China.